



MODIS/VIIRS ST Meeting, BWI, Maryland, May 14-16, 2008

MODIS C4/C5 LST Status Report and Proposed C6 Processing Plan

Zhengming Wan
University of California, Santa Barbara



Basic Considerations in MODIS LST Algorithms

1. LST is retrieved from TIR data only in clear-sky conditions.
LST is not mixed with cloud-top temperature in the atmospheric product (TIR signal from surface cannot penetrate clouds to reach satellites).
2. LST is defined by the radiation emitted by the land surface observed by MODIS at the instantaneous viewing angle.
Applications may need LST at different angles (nadir or 50° from nadir).
3. Proper resolving of the **land-atmosphere coupling** is the key in retrieving surface & atmospheric properties.
Integrated retrieval is possible but it takes a lot of computing time.
Use multi-bands in the atmospheric windows for the LST retrieval.
The values of atmospheric temperature and water vapor are useful to improve the LST retrieval. However, there may be large errors in these values. Use them as indicates of ranges or initial guesses only.
4. Input data: MOD021KM, MOD03, MOD07, MOD10, MOD12, MOD35 & MOD43.

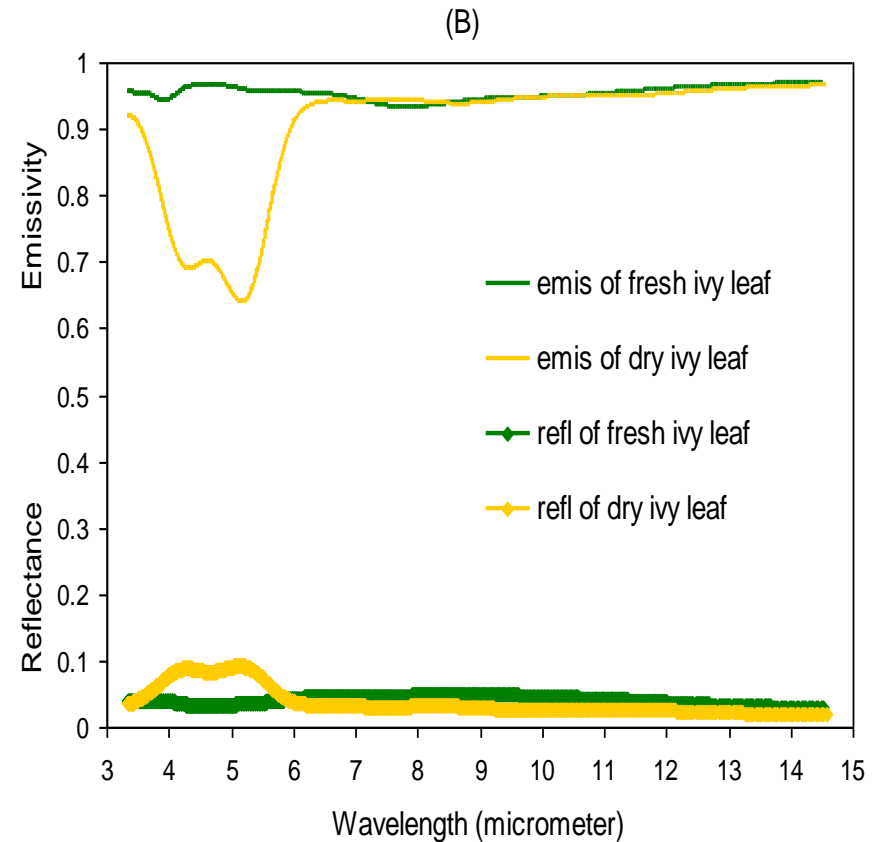
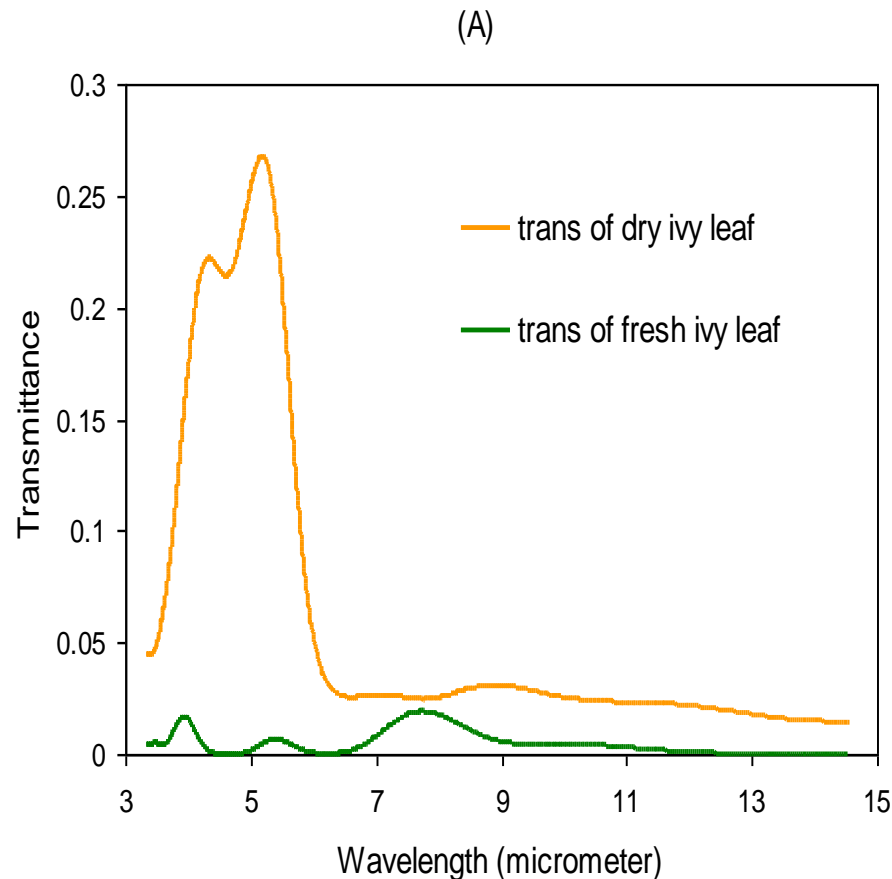
Basic Considerations in MODIS LST Algorithms (II)

5. The standard MODIS cloudmask product (MOD35 and MYD35) is used because it is one of the best cloudmask products available and it is good in most cases ($> 98\%$). However, mismasking (cloudy pixels as clear-sky pixels at 99% confidence, or clear pixels at 99% confidence as uncertainly clear) exist in all cloudmask products. Therefore, it is important to properly use this cloudmask product and remove LSTs under effects of cloud contaminations after the initial LST generation in the production system.
6. The split-window LST algorithm is the primary algorithm used to generate the MODIS LST products including the level-2 product (MOD11_L2 and MYD11_L2) and the 1km level-3 product (MOD11A1 and MYD11A1) because the surface emissivities vary within narrow ranges in the spectral ranges of MODIS bands 31 and 32 for all land-cover types but at different widths.
7. Surface emissivities do not significantly change with time because thermal infrared radiation almost does not penetrate a thin vegetation leaf and its reflectance does not change with the water content in the leaf in the spectral range above $7\mu\text{m}$ and the skin of sands and soil lands always stay in dry condition normally in clear-sky days.





Transmittance (in plot A), reflectance and emissivity (both in plot B) spectra of a single ivy leaf (about 0.18 mm thick) in fresh and extremely dry conditions from measurements with a spectroradiometer and integral sphere system by the UCSB MODIS LST group





Major refinements implemented in the V5 daily LST code (PGE16)

Specification / Action	in V4	in V5
grid size of LST/emissivities in M*D11B1 retrieved from the day/night algorithm	5km x 5km (exactly 4.63km)	6km x 6km (exactly 5.56km)
number of sub-ranges of zenith view angles	5 for the whole scan swath	2x8 for the whole scan swath
effect of slope in the M*D11B1 grid	not considered	considered in the QA
temporal averaging in the 1km LST product	yes	no
option of combined use of Terra and Aqua data in the day/night algorithm	no	yes
incorporate the split-window method into the day/night algorithm	partially with landcover-based em31, em32 and initial Ta, cwv	fully with em31, em32, Ta and cwv as variables in the iterations
clear-sky pixels defined by MODIS cloudmask	at 99% confidence over land at 66% confidence over lakes	at 99% confidence over snow/ice at confidence of $\geq 95\%$ over non-snow/ice land $\leq 2000\text{m}$ at confidence of $\geq 66\%$ over non-snow/ice land $> 2000\text{m}$ at confidence of $\geq 66\%$ over lakes
removing cloud-contaminated LSTs	not implemented	implemented for M*D11A1 and M*D11B1
empirical optical-leak correction to band 32	not implemented	made for the last four pixels each scan line in Terra MODIS L1B granules



Remove cloud-contaminated LSTs in C5 level-3 LST products with constraints (δT) on the temporal variations in clear-sky LSTs (in PGE16C)

δT (K)	Description of land-cover (type #)
3.0	water (0)
7.6	evergreen needleleaf forest (1)
7.2	evergreen broadleaf forest (2)
7.2	deciduous needleleaf forest (3)
7.0	deciduous broadleaf forest (4)
7.0	mixed forest (5)
8.0	closed shrublands (6)
9.0	open shrublands (7)
8.4	woody savannas (8)
9.0	savannas (9)
9.0	grasslands (10)
5.0	permanent wetlands (11)
8.0	croplands (12)
8.0	urban and built-up (13)
8.0	cropland and mosaics (14)
4.0	snow and ice (15)
11	bare soil and rocks (16)
10	unclassified (17)

- In step 1, remove the worst LSTs that are different from the 32-day maximum by more than 4 times the δT value or different from the 16-day maximum by more than 3 times the δT value.

- In step 2, remove the LSTs that are different from the 8-day maximum by more than 2 times the δT value, then calculate the 8-day average value of the remaining LSTs.

- In step 3, remove the LSTs that are different from the 8-day average value by more than the δT value.

- In order to consider the larger natural temporal changes in clear-sky LSTs in the growing and drying seasons, and in cold regions, the δT values are adjusted on the basis of statistical values of mean and standard deviation of LSTs in four periods of 8 days for each land-cover type in the tile under processing.

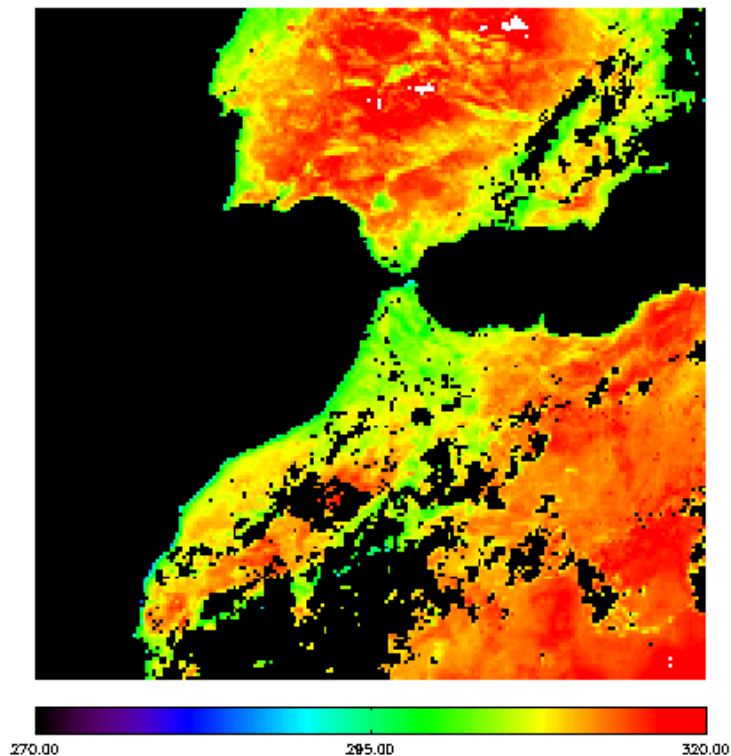
This scheme may not work well in wet regions because few clear-sky days with valid LSTs exist there.



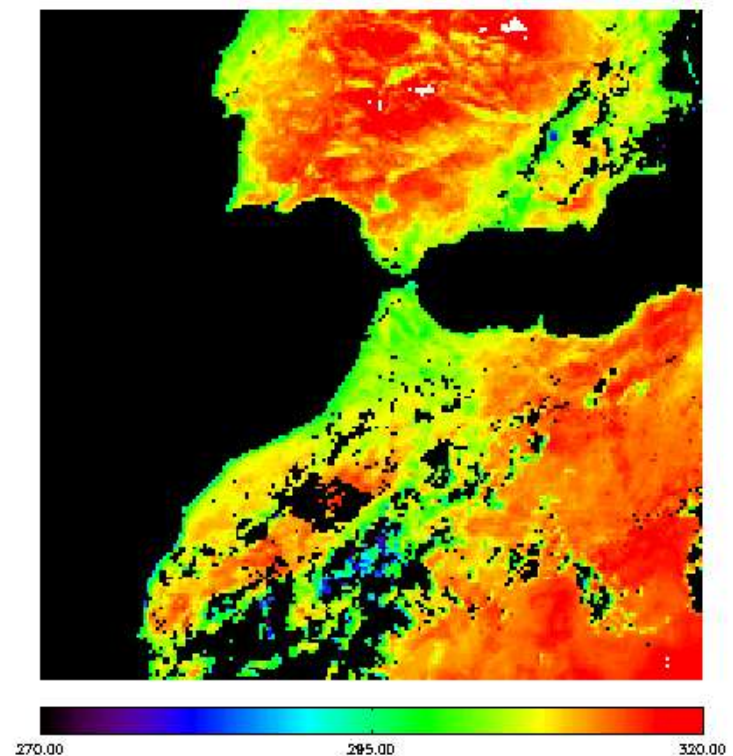
Improvements of the C5 LST Products over C4

Cloud-contaminated LSTs were removed in level-3 C5 LST products. Daytime LSTs in MOD11B1.A2003203.h17v05 (7/22/03) are shown below. The minimum daytime LST value is 264.68K in the right image (C4) or 284.26K in the left image (C5). Note that cloud-contaminated LSTs in the C5 level-2 LST products are not removed yet.

C5

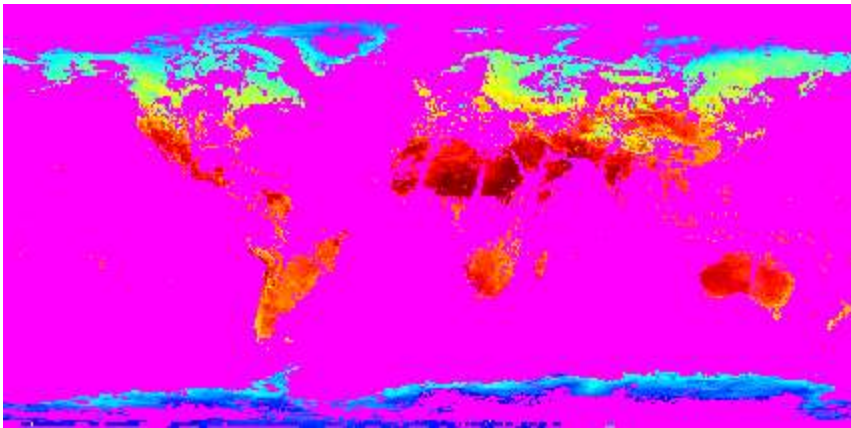


C4

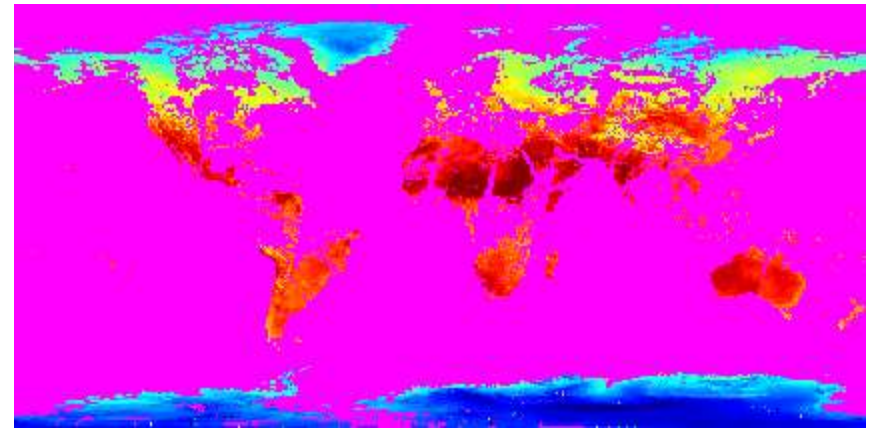


Comparison of the C4 and C5 CMG LST Products (M*D11C)

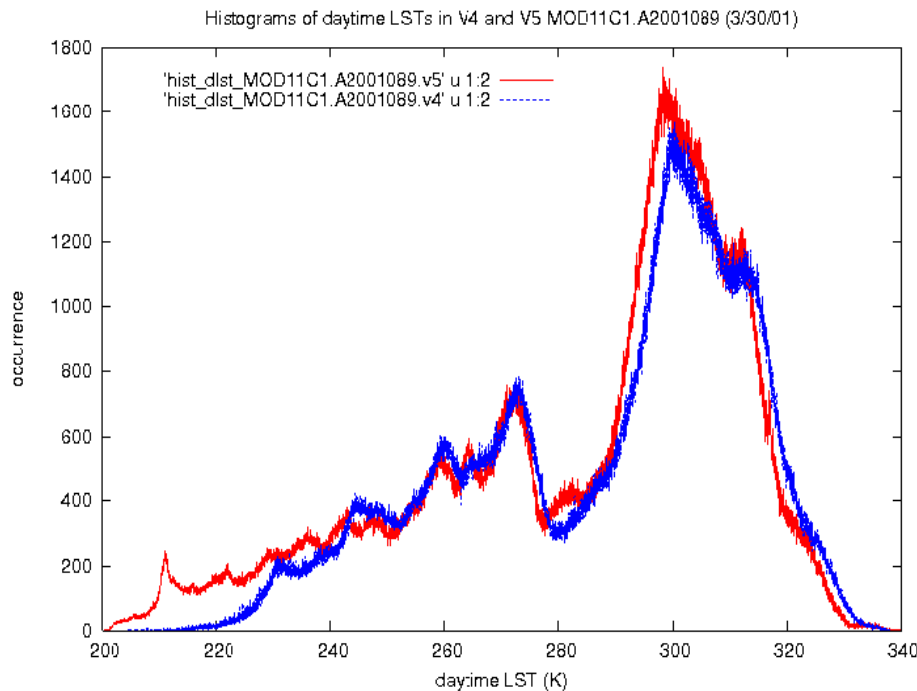
The LSTs in M*D11C products are based on the LSTs retrieved by the day/night algorithm and supplemented by the LSTs retrieved by the split-window algorithm.



LST_day in C4 MOD11A1.A2001089



LST_day in C5 MOD11A1.A2001089 (3/30)



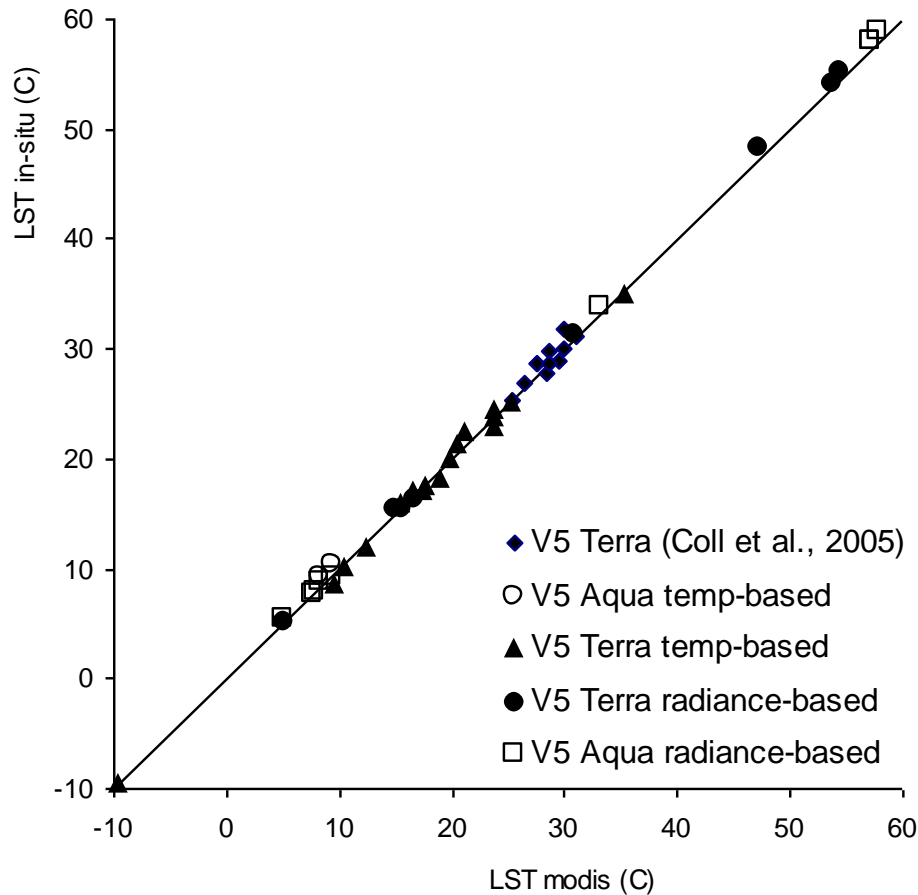
Highlights:

- C4 & C5 daytime LSTs have different spatial distributions because V4 & V5 PGEs use C4 & C5 MODIS cloudmask products.
- The mean and standard deviation of the differences between LSTs retrieved by the two algorithms are less than 0.2K and 0.5K in V5 so the 6km LSTs from the day/night algorithm can be validated in-directly.
- However, they are larger (about 1.5K and 1.8K) in V4 (the effects of aerosol and cloud contaminations propagate into clear-sky days thru the initialization with the affected lower emis values in the V4 day/night algorithm).



Validation of the C5 LST Products generated in V5 tests

By comparisons of LST values in the C5 MOD11_L2 and MYD11_L2 products with the in-situ values in Wan et al., 2002; Wan et al., 2004; Coll et al., 2005, and radiance-based validation results over Railroad Valley, NV in June 2003 and a grassland in northern TX in April 2005. LST errors < 1K in most cases.



Notes for applications of C4 & C5 LST products:

- In M*D11_L2, if valid LSTs are available in both C4 & C5, their difference is less than 0.2-0.4K in most cases.
- In M*D11A1 within latitude 28°(MODIS orbits w/o overlapping), if valid LSTs are available in both C4 & C5, their difference is less than 0.2-0.4K in most cases. Outside the latitude region, if valid LSTs are available in both C4 & C5 and at the same view time (indicating temporal average not applied in C4), their difference is less than 0.2-0.4K in most cases. Users should remove cloud-contaminated LSTs in the C4 product before using them in applications.
- LSTs severely contaminated by clouds were removed from level-3 C5 products, but not from all C4 products. It is very difficult to remove such LSTs from the 8-day C4 M*D11A2 products because the cloud contamination effect may be reduced in the 8-day averaging.

See details in Wan (2008) and Wan and Li (2008)



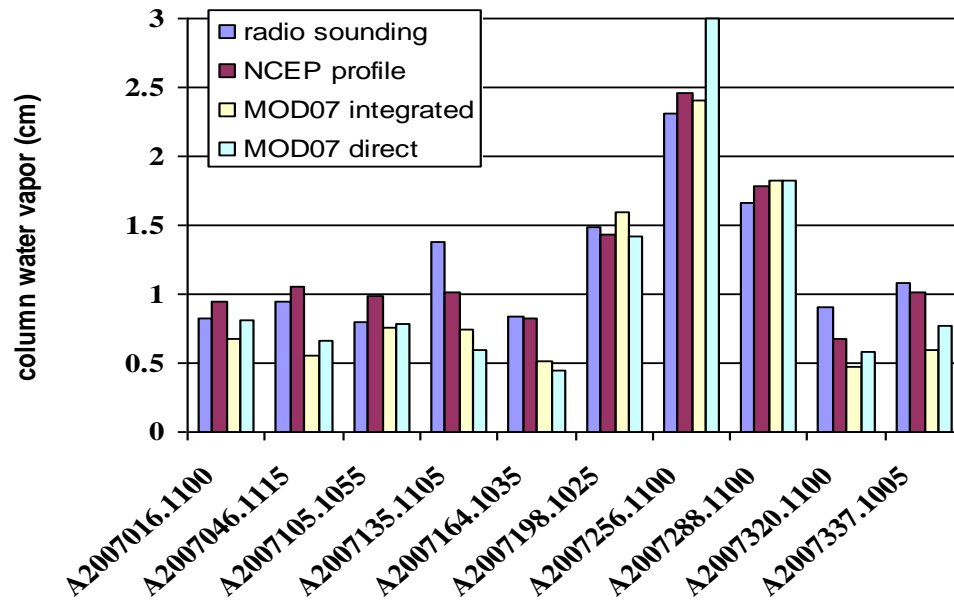
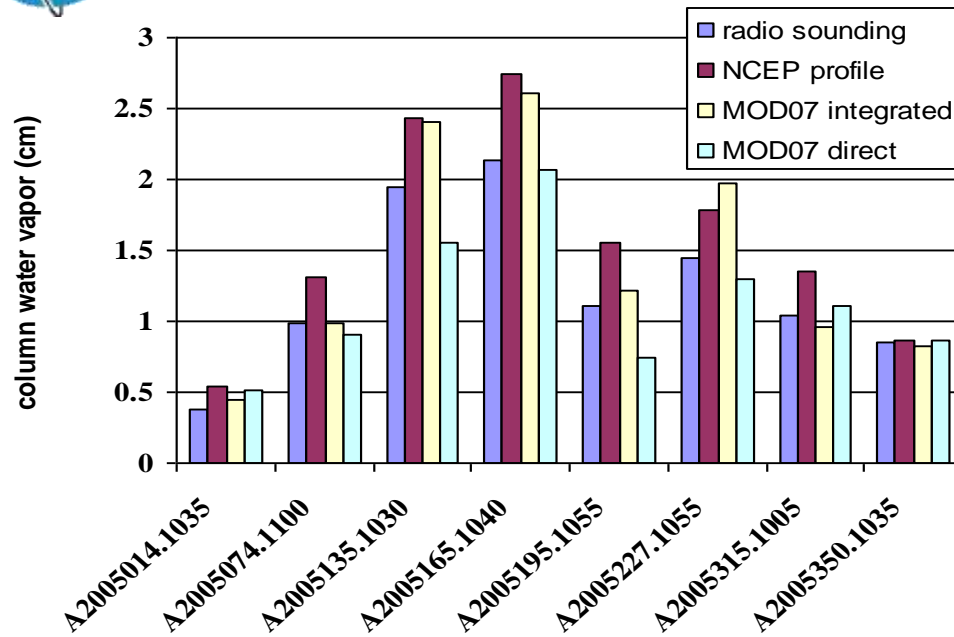
Institute for
Computational Earth System Science
University of California, Santa Barbara

Radiance-based approach to valid LSTs

1. It uses measured or estimated surface emissivity spectra, and atmospheric water vapor and temperature profiles in atmospheric radiative transfer (RT) simulations to invert the band-31 brightness temperature (Tb31) of the MODIS observation to a LST value, and compare this value with the LST value in the MOD11 product.
2. This approach has been validated by comparisons to the conventional temperature-based approach in large homogeneous fields (lakes, grassland, and rice fields) by the MODIS LST group and César Coll's group.
3. It is better than the conventional temperature-based approach because of the large spatial variation in LSTs especially in the daytime and the small horizontal variations in atmospheric temperature and water vapor profiles in clear-sky and flat areas.
4. It is important to use the atmospheric profiles appropriate to MODIS observations by constraints of time (within 2 hours) and distance ($\leq 100\text{km}$).
5. It is important to perform the R-based approach on a series of days and check the quality with (Tb31 – Tb32) values: in successful RT simulations not only Tb31 but also Tb32 of MODIS observations should be well matched simultaneously.
6. The NCEP atmospheric profiles may be used In the R-based validation **with care**.
7. **The R-based approach has larger uncertainties in wet conditions and it does not work well if the atmospheric profile used in the atmospheric RT simulation is significantly different from the real atmospheric state along the path of MODIS observation. This is the same problem faced by all the T/E methods in the atmospheric correction for extracting emissivity spectra (Li et al., 1999).**



Changes of column water vapor (cwv) over In-salah, Algeria (27.22°N, 2.5°E) during Jan. – Dec. in 2005 and 2007



(1) There is a larger seasonal variation in cwv over this desert site in 2005.

(2) The cwv values provided by two methods (integrated and direct) in MOD07_L2 may be quite different, especially in the wet year 2005.

(3) The cwv values calculated from NCEP modeled profiles are larger than the values calculated from radio sounding profiles (12Z) by 23-42% in the first 7 cases of 2005. But the difference is smaller in most cases of 2007. Therefore, we should be very careful about the large errors in NCEP profiles in wet conditions.

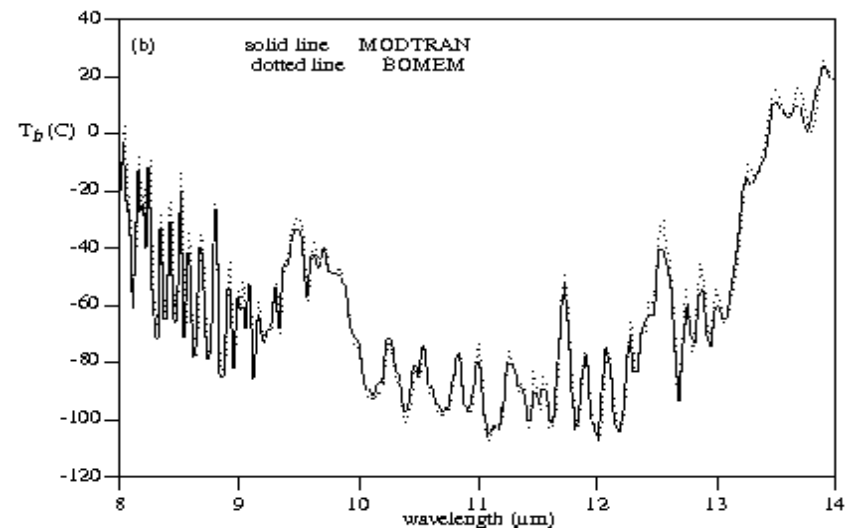
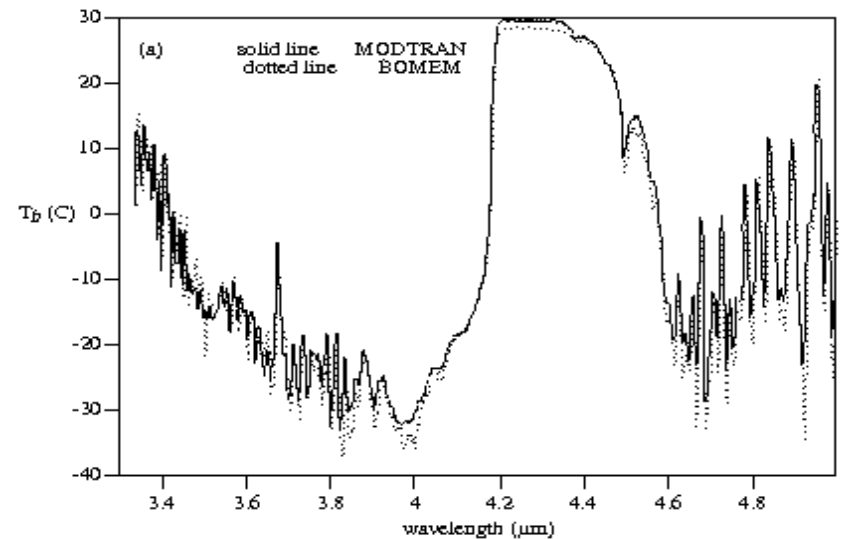
(4) If there are large temporal variations in the surface emissivities retrieved from satellite TIR data over the desert site, the major source of errors may be in the process of atmospheric correction, especially when NCEP modeled profiles are used in relatively wet conditions.



High quality of the Bomem TIR spectroradiometer (MR100) and MODTRAN simulations



Above, The Bomem TIR spectroradiometer (MR100) was deployed in Railroad Valley, NV in June 2003. It is similar to the instrument used to validate the MODIS SST product. Right, Brightness temperature (T_b) of downwelling radiance at nadir measured by the TIR spectroradiometer at 10:30 PDT 6/29/03 in Railroad Valley and the T_b calculated by MODTRAN4 based on measured atmospheric profiles.



Comparison between temperature-based (in-situ LST) and radiance-based (TOA L31 inverted LST) validations for the Terra MODIS LST product at the rice field in Valencia, Spain, in six ideal clear-sky cases in 2003-2004 (Coll et al., 2005). The atmospheric temperature and water vapor profiles used in the radiance-based validation were measured by radio sounding in Murcia, Spain (38.0° N, 1.17° W), about 160km south of Valencia. The mean and standard deviation of the differences between the in-situ LST and TOA L31 inverted LST values in these ideal clear-sky cases are 0.03K and 0.37K, respectively. **The radiance-based approach is also validated by César Coll with more in-situ LSTs and atmospheric profiles measured by radiosode balloons launched at the site in multiple years.**

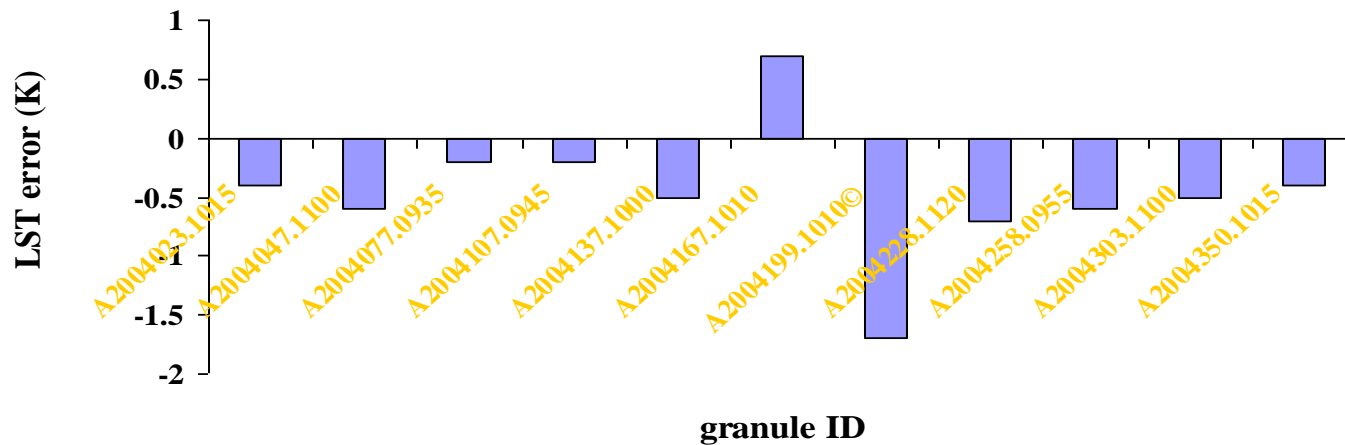
case no.	Granule ID	date & time (m/d hh:mm)	viewing zenith angle (°)	radiosonde cwv, Ts-air (in MOD07) (cm, K)	MODIS LST (δT) (K)	in-situ LST (K)	TOA L31 inverted LST (K)	profile-based Tb31-Tb32 (K)	MODIS Tb31 - Tb32 (K)
1	2003192.1040	7/11 10:42	27.7	1.98, 309.5 (2.16,302.4)	302.7 (0.3)	302.1	302.7	0.23	0.44
2	2003224.1040	8/12 10:42	28.1	1.40, 306.8 (1.46,297.5)	304.3 (0.1)	304.4	304.1	0.05	0.49
3	2004190.1020	7/08 10:24	50.3	1.15, 302.8 (1.56,294.4)	298.6 (0.5)	298.5	298.9	0.14	0.52
4	2004209.1050	7/27 10:54	6.0	2.09, 307.1 (1.84,296.9)	301.5 (0.2)	301.1	301.2	0.17	0.56
5	2004216.1100	8/03 11:00	6.0	2.18, 308.0 (2.34,298.5)	303.1 (0.2)	303.2	302.8	0.34	0.78
6	2004225.1050	8/12 10:54	5.7	2.22, 306.9 (1.94,298.5)	301.9 (0.1)	301.9	301.7	0.26	0.58

Radiance-based validation of V5 Terra MODIS LSTs at the CarboEurope site in Hainich, Germany (51.0792°N, 10.4522°E). The atmospheric temperature and water vapour profiles used in the radiance-based validation were measured by radio sounding in Meiningen, Germany (50.56°N, 10.38°E), about 60km south of Hainich. In column 6, (δT)_n indicates the standard deviation of MODIS LSTs in n pixels with valid LSTs in the four pixels surrounding the site. The mean and RMS of errors (in column 8) are -0.3K and 0.73K. **This set of validation results clearly indicates that the LST cannot be validated by longwave radiation data measured at 44m above surface as Wang et al did for the same site in a recent paper published in Remote Sensing of Environment, v112, 623-635, 2008 (bias -2.2K and RMSE 2.5K)**

case no.	Granule ID	local solar date & time (d/m h:m)	viewing zenith angle (°)	Radiosonde cwp, T_{s-air} and values in (M*D07) (cm, K)	MODIS LST (δT) _n (K)	MOD L31 inverted LST (K)	LST _{modis} - MOD L31 inverted LST (K)	profile-based Tb31- Tb32 (K)	MODIS Tb31- Tb32 (K)	column 10 - column 9 (K)
1	A2004021.2135	21/1 22:22	41.0	0.37,268.3 (0.46,265.3)	264.2 (1.69)3	265.0	-0.8	-0.23	-0.14	0.09
2	A2004023.1015	23/1 10:57	20.8	0.70,268.1 (0.65,269.1)	269.1 (0.62)2	269.5	-0.4	-0.14	0.07	0.21
3	A2004046.2130	15/2 22:12	34.3	0.90,274.4 (0.92,274.0)	273.0 (---)0	273.3	-0.3	-0.13	-0.04	0.09
4	A2004047.1100	16/2 11:42	43.6	0.72,276.8 (0.96,276.4)	276.6 (0.51)4	277.2	-0.6	-0.10	-0.10	0.0
5	A2004077.0935	17/3 10:17	56.9	0.74,286.2 (0.94,284.3)	285.3 (0.88)4	285.5	-0.2	-0.21	0.16	0.37
6	A2004077.2045	17/3 21:27	26.3	1.22,281.2 (1.34,282.9)	282.7 (0.45)4	283.6	-0.9	-0.10	-0.35	-0.25
7	A2004107.0945	16/4 10:27	48.3	1.02,288.0 (1.00,284.9)	292.5 (0.55)4	292.7	-0.2	0.40	0.69	0.29
8	A2004107.2100	16/4 21:42	9.8	0.89,282.2 (1.06,279.8)	280.7 (0.64)4	280.9	-0.2	-0.17	-0.22	-0.05
9	A2004135.2125	14/5 22:07	26.5	1.08,281.2 (1.09,278.7)	279.8 (0.22)4	279.7	0.1	-0.12	-0.01	0.11
10	A2004137.1000	16/5 10:42	36.1	1.03,286.8 (1.60,286.0)	288.5 (0.37)4	289.0	-0.5	0.22	0.36	0.14
11	A2004166.2040	14/6 21:22	33.5	2.28,288.0 (3.25,286.3)	286.4 (0.29)4	286.1	0.3	0.30	0.60	0.30
12	A2004167.1010	15/6 10:52	21.3	2.00,294.2 (3.39,291.0)	293.7 (0.76)3	293.0	0.7	0.43	1.00	0.57
13	A2004198.2040	16/7 21:22	33.4	2.20,288.6 (3.09,288.3)	288.5 (0.53)4	287.8	0.7	0.07	0.34	0.27
14	A2004199.1010	17/7 10:52	21.2	2.62,298.0 (2.94,294.9)	296.2 (1.44)4©	297.9	-1.7	0.98	0.86	-0.12
15	A2004228.1120	15/8 12:02	56.5	2.00,293.2 (2.59,291.9)	290.8 (1.51)3	291.5	-0.7	0.42	0.83	0.41
16	A2004228.2050	15/8 21:32	18.2	1.67,287.8 (2.33,285.7)	287.1 (0.09)4	285.5	1.6	-0.20	0.51	0.71
17	A2004258.0955	14/9 10:37	42.5	2.23,291.0 (2.35,288.7)	289.1 (0.83)3	289.7	-0.6	0.80	0.85	0.05
18	A2004262.2040	18/9 21:22	33.3	1.22,283.0 (2.05,287.6)	286.3 (0.27)4	286.9	-0.6	-0.08	0.03	0.11
19	A2004292.0940	18/10 10:22	52.3	1.10,281.2 (0.94,280.0)	280.5 (0.60)3	282.0	-1.5	0.23	-0.08	-0.31
20	A2004292.2050	18/10 21:32	18.0	0.78,278.6 (0.88,271.1)	278.7 (0.41)4	278.8	-0.1	-0.15	-0.05	0.10
21	A2004303.1100	29/10 11:42	43.4	1.41,287.2 (1.61,285.5)	287.0 (0.51)4	287.5	-0.5	0.22	0.32	0.10
22	A2004303.2035	29/10 21:17	39.6	1.72,281.8 (1.30,280.1)	279.7 (0.43)4	279.6	0.1	-0.06	0.18	0.24
23	A2004350.1015	15/12 10:57	12.8	0.48,268.1 (0.59,275.9)	271.8 (0.89)4	272.2	-0.4	-0.26	-0.26	0.0
24	A2004350.2130	15/12 22:12	34.1	0.85,268.5 (0.67,273.8)	271.0 (0.44)4	271.0	0.0	-0.36	-0.28	0.08

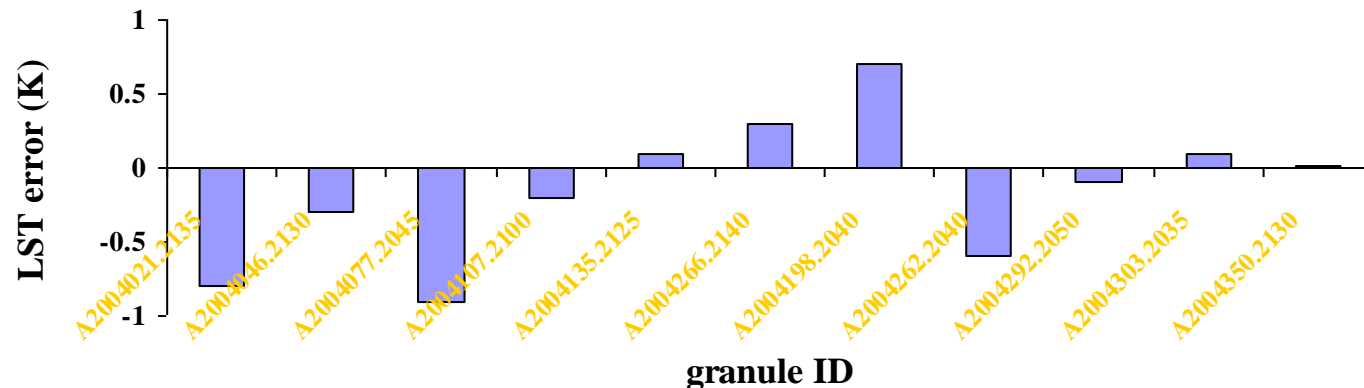


**Radiance-based validation of LSTs in the V5 MOD11_L2
product at Hainich, Germany (51.0972D N, 10.4522D E).
Daytime LSTs range from 272-293K.**



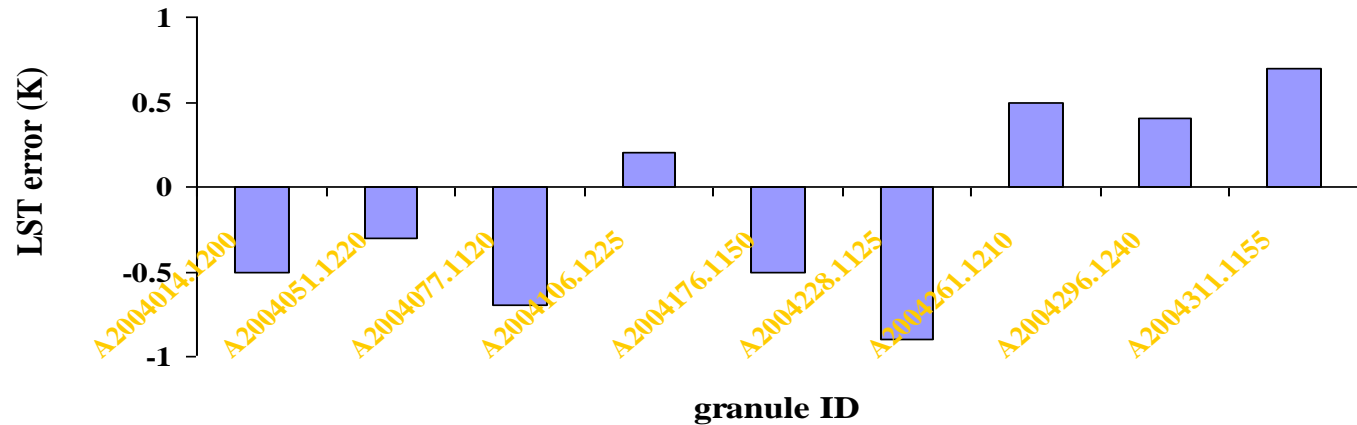
with radio
sounding
profiles

**Radiance-based validation of LSTs in the V5 MOD11_L2 product
at Hainich, Germany (51.0972D N, 10.4522D E).
Nighttime LSTs range from 265-288K.**



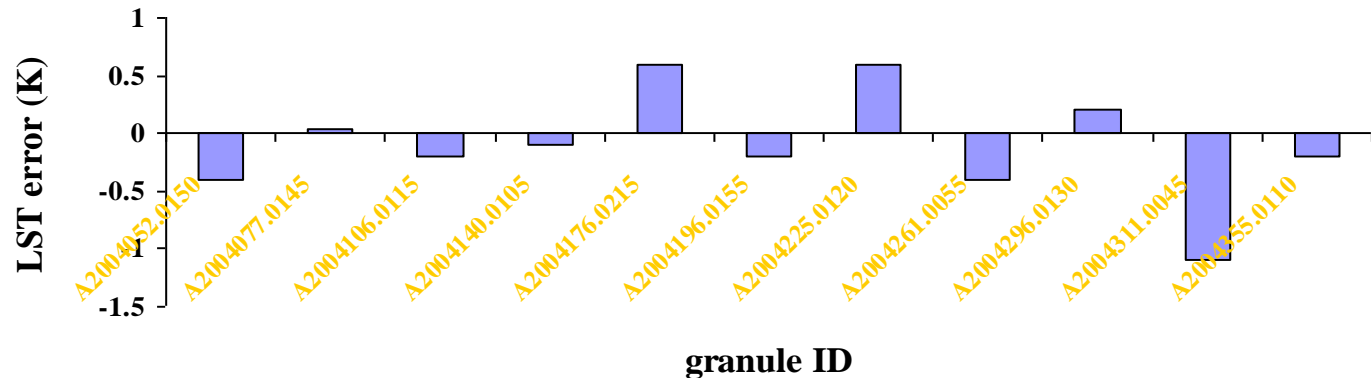


**Radiance-based validation of LSTs in the V5 MYD11_L2 product at Hainich, Germany (51.0972D N, 10.4522D E).
Daytime LSTs range from 273-295K.**



with radio
sounding
profiles

**Radiance-based validation of LSTs in the V5 MYD11_L2 product at Hainich, Germany (51.0972D N, 10.4522D E).
Nighttime LSTs range from 267-290K.**

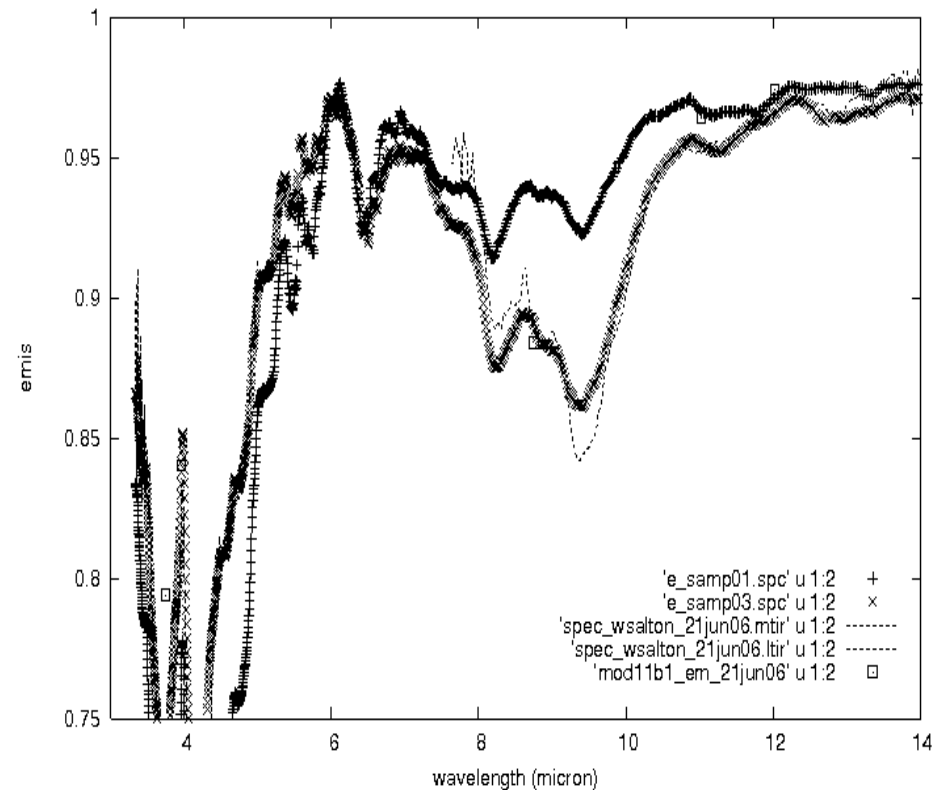
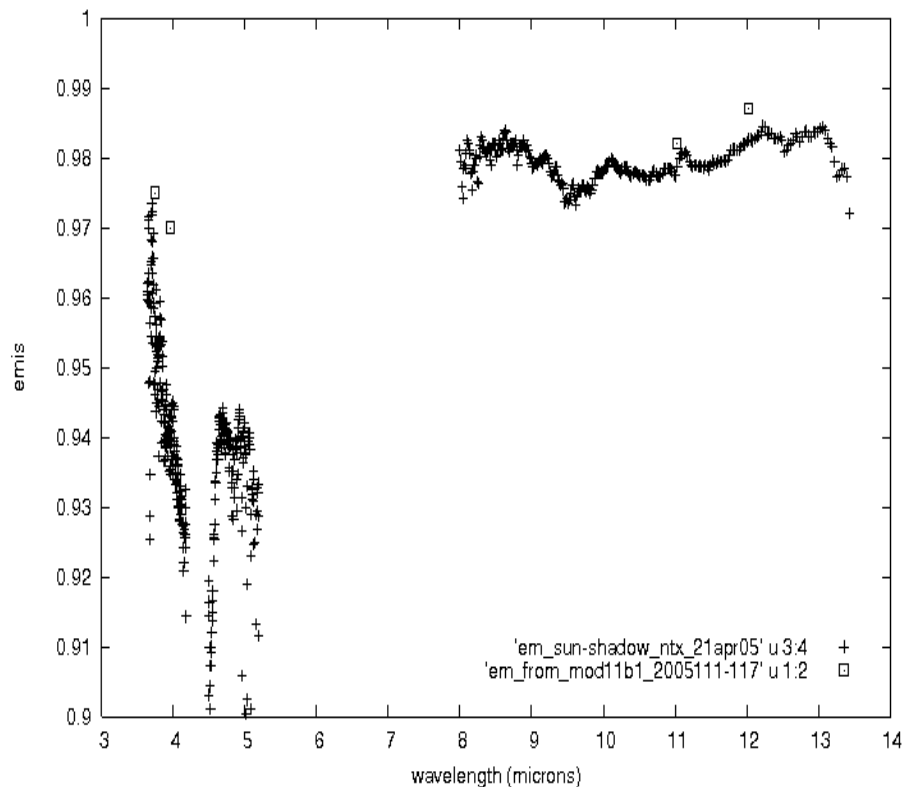


Radiance-based validation of V5 Terra (labelled as T in column 2) and Aqua (labelled as A in column 2) MODIS LSTs at the validation sites in Railroad Valley, Nevada (38.4817°N, 115.6905°W) in cases 1-10 and grassland, Texas (36.2992°N, 102.5706°W) in cases 11-14. M*D07 in column 5 represents the atmospheric temperature and water vapour product MOD07 from Terra MODIS data or MYD07 from Aqua MODIS data.

case no.	Granule ID (T/A)	local solar date & time (m/d h:m)	viewing zenith angle (°)	radiosonde cwv, Ts-air (M*D07) (cm, K)	MODIS LST (δT) (K)	MOD L31 inverted LST (K)	LST _{modis} - MOD L31 inverted LST (K)	profile-based Tb31-Tb32 (K)	MODIS Tb31-Tb32 (K)
1	A2003177.1800 (T)	6/26 10:19	53.7	0.71,298.2 (0.56,299.5)	320.4 (1.4)	321.5	-1.1	0.15	0.23
2	A2003178.1840 (T)	6/27 11:02	11.5	0.78,299.7 (0.93,304.2)	326.8 (1.7)	327.6	-0.8	0.03	0.21
3	A2003179.0545 (T)	6/27 22:06	4.6	1.00,289.2 (1.04,287.4)	288.6 (0.6)	288.7	-0.1	-0.48	-0.47
4	A2003180.1830 (T)	6/29 10:50	12.0	0.84,305.2 (1.35,305.2)	327.5 (1.4)	328.5	-1.0	0.08	0.11
5	A2003181.0535 (T)	6/29 21:54	18.4	0.89,295.2 (0.55,290.4)	289.8 (0.6)	289.8	0.0	-0.59	-0.37
6	A2003177.1010 (A)	6/26 02:28	46.9	0.71,288.2 (0.46, 283.8)	281.0 (0.7)	281.1	-0.1	-0.78	-0.70
7	A2003178.2020 (A)	6/27 12:37	44.4	0.78,302.7 (0.41, 293.6)	330.3 (1.5)	331.1	-0.8	0.36	0.55
8	A2003179.0955 (A)	6/28 02:16	31.9	0.90,284.2 (0.76, 286.2)	281.6 (0.4)	282.0	-0.4	-0.66	-0.48
9	A2003180.2005 (A)	6/29 12:25	55.7	0.84,305.2 (0.84, 297.7)	326.5 (1.8)	327.3	-0.8	0.38	0.69
10	A2003181.0945 (A)	6/30 01:54	11.4	0.74,295.2 (0.40, 288.0)	282.5 (0.5)	282.4	0.1	-0.69	-0.53
11	A2005111.1755 (T)	4/21 11:05	22.0	0.35, 289.5 (0.46,289.4)	304.1 (0.4)	304.6	-0.5	-0.07	0.01
12	A2005112.0455 (T)	4/21 22:09	5.84	0.84, 282.2 (0.62,279.4)	278.3 (0.2)	278.5	-0.2	-0.26	-0.40
13	A2005111.1930 (A)	4/21 12:40	44.9	0.58, 293.2 (0.50,288.4)	306.5 (0.1)	307.1	-0.6	0.19	0.33
14	A2005112.0910 (A)	4/22 02:20	40.5	0.84, 280.2 (0.65,278.9)	278.4 (0.1)	278.6	-0.2	-0.28	-0.27



Emissivity spectra of the grassland in TX on 21 April 2005 (left) and a bare soil site near Salton Sea, CA on 21 June 2006 (right) measured by the sun-shadow method with the Bomem TIR spectroradiometer and comparisons to band emissivities in the V5 MOD11B1 product

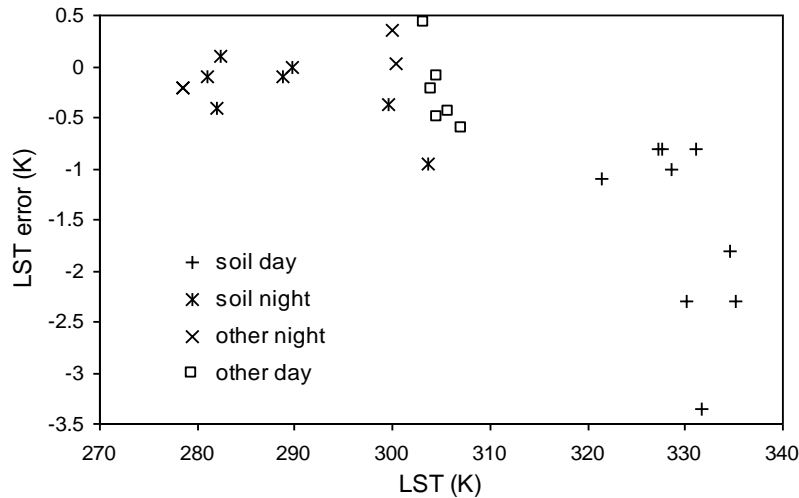


Radiance-based validation of V5 Terra and Aqua MODIS LSTs at the validation sites in Salton Sea (33.2°N, 115.75°W) in cases 1-6 and nearby bare soil land (33.25°N, 115.95°W) in cases 7-12. The δT value in column 6 is the standard deviation of MODIS LSTs in the four pixels surrounding the validation site.

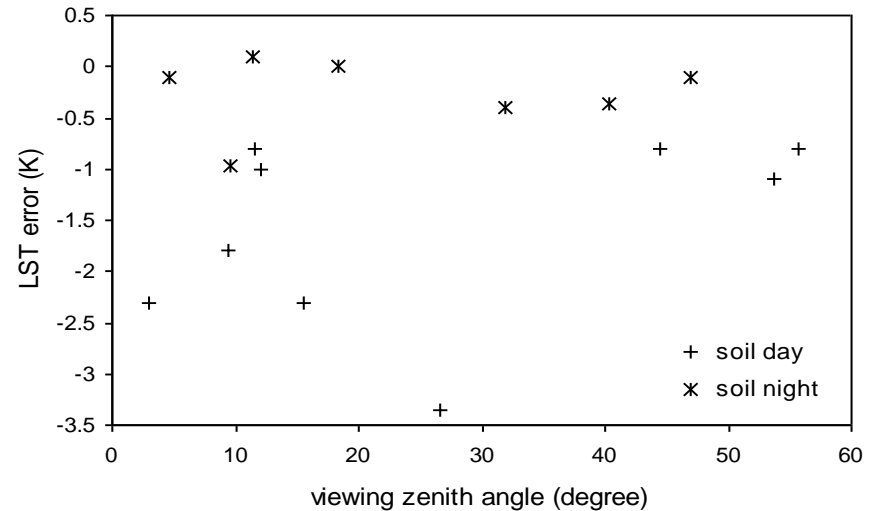
case no.	Granule ID (T/A)	local solar date & time (m/d h:m)	viewing zenith angle (°)	radiosonde cwv, Ts-air (M*D07) (cm, K)	MODIS LST (δT) (K)	MOD L31 inverted LST (K)	$LST_{modis} - MOD L31$ inverted LST (K)	profile-based Tb31-Tb32 (K)	MODIS Tb31-Tb32 (K)
1	A2006171.0545 (T)	6/19 22:04	8.2	1.95,300.3 (1.67,303.1)	300.4 (0.04)	300.4	0.0	0.37	0.31
2	A2006171.1000 (A)	6/20 02:19	41.4	1.95,300.3 (1.47,301.5)	300.3 (0.07)	299.9	0.4	0.40	0.45
3	A2006171.2100 (A)	6/20 13:20	16.9	1.61,308.2 (1.13,303.4)	304.5 (0.1)	304.6	-0.1	0.45	0.49
4	A2006172.1830 (T)	6/21 10:51	1.3	1.12,309.9 (0.79,302.9)	303.9 (0.06)	304.1	-0.2	0.32	0.33
5	A2006173.2050 (A)	6/22 13:08	8.0	1.63,312.2 (0.83,303.6)	305.4 (0.13)	305.8	-0.4	0.55	0.46
6	A2006174.1820 (T)	6/23 10:38	25.2	2.56,308.2 (3.65,304.8)	303.6 (0.23)	303.2	-0.4	1.14	1.39
7	A2006171.0545 (T)	6/19 22:03	9.6	1.95,305.2 (1.33,304.4)	302.6 (0.15)	303.6	-1.0	-0.28	-0.55
8	A2006171.1000 (A)	6/20 02:19	40.4	1.95,300.3 (1.26,300.3)	299.1 (0.29)	299.5	-0.4	-0.39	-0.51
9	A2006171.2100 (A)	6/20 13:20	15.5	1.61,315.2 (1.00,297.6)	332.9 (0.25)	335.2	-2.3	0.92	0.81
10	A2006172.1830 (T)	6/21 10:50	3.0	1.12,309.9 (0.60,309.0)	327.8 (0.25)	330.1	-2.3	0.15	-0.06
11	A2006173.2050 (A)	6/22 13:08	9.5	1.63,312.2 (1.05,298.5)	332.7 (0.2)	334.5	-1.8	1.02	1.14
12	A2006174.1820 (T)	6/23 10:37	26.6	2.56,308.2 (3.11,313.1)	328.2 (0.15)	331.6	-3.4	2.13	2.08

Error Analysis of the LSTs Retrieved by the Split-window Method

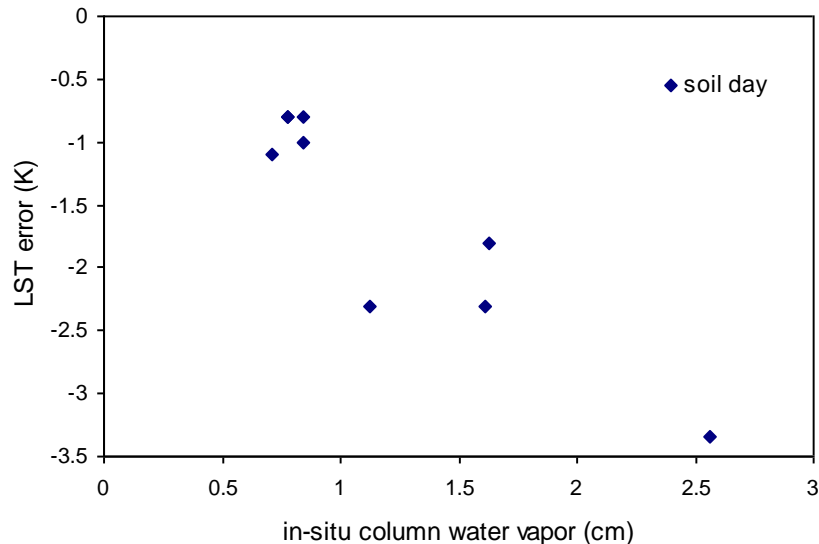
(A)



(B)



(C)

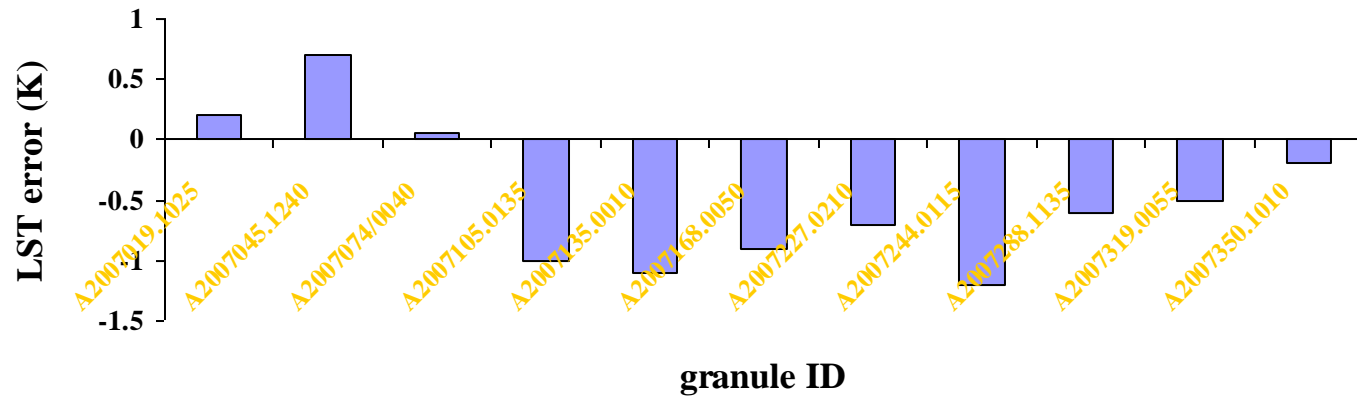


The LST errors versus LST values shown in the last two tables in two groups, one for soil sites in Railroad Valley and near Salton Sea, and another for the grassland and lake sites, in day and night cases, respectively (A). The LST errors versus viewing zenith angle for the cases in the soil group (B), and the LST errors versus column water vapor from measured atmospheric profiles for the cases in the soil day group (C).

The reason for larger errors in high LST cases with $cwv > 1.5\text{cm}$ is that the range of $T_s - \text{air}$ 16K for the LST values used in the development of the split-window algorithm is not wide enough for the daytime bare soil cases.

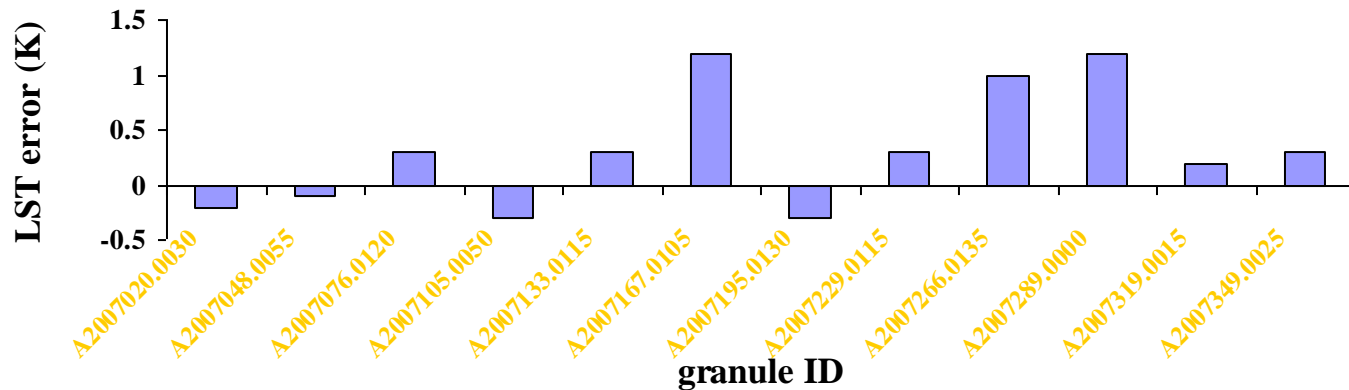


**Radiance-based validation of LSTs in the V5 MOD11_L2 product
at a site (89.95D S, 0.05D E) near the South Pole.
LSTs range from 201-244K.**



with radio
sounding
profiles

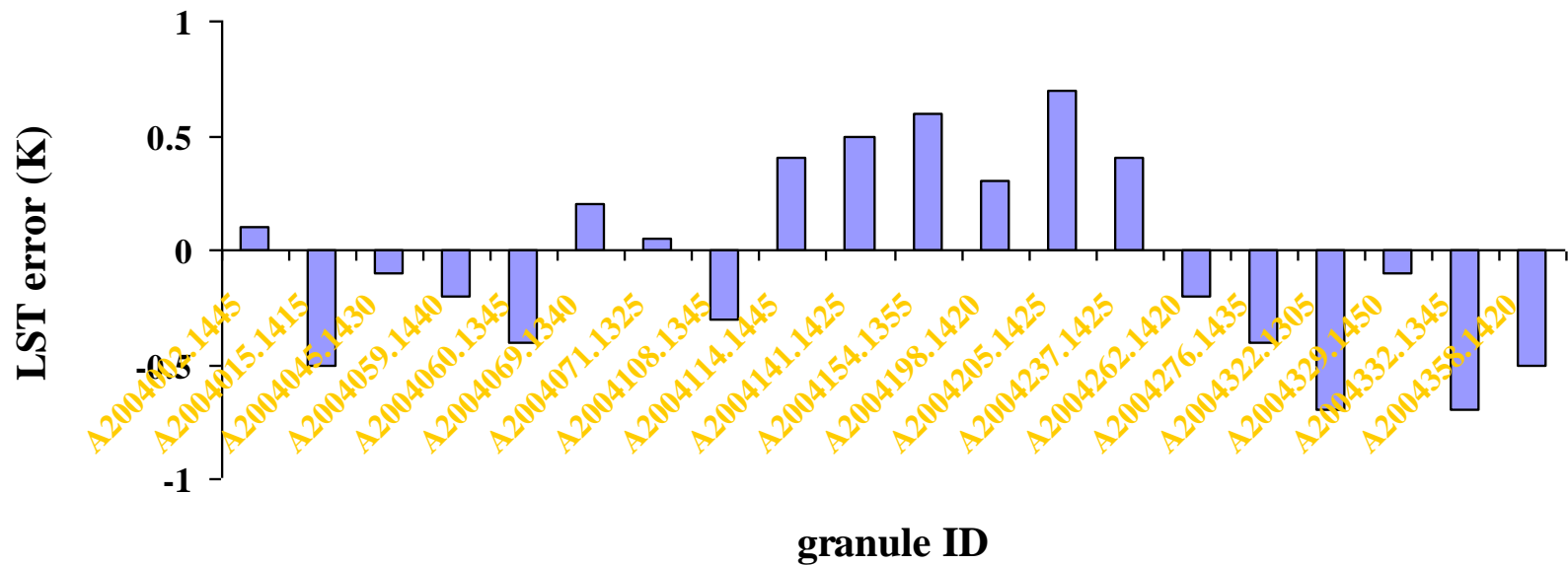
**Radiance-based validation of LSTs in the V5 MOD11_L2 product
at Cherskij, Russian (68.75D N, 161.27D E).
LSTs range from 235-291K.**





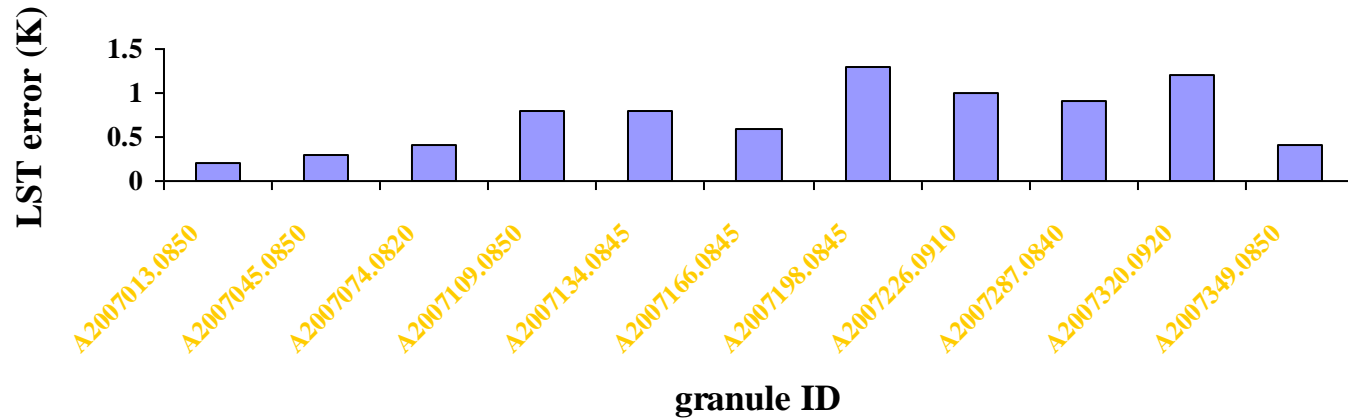
with NCEP modeled profiles

Radiance-based validation of LSTs in the V5 MOD11_L2 product at DYE-2,
Greenland (66.481D N, 46.28D W).
Daytime LSTs range from 217 - 272K.



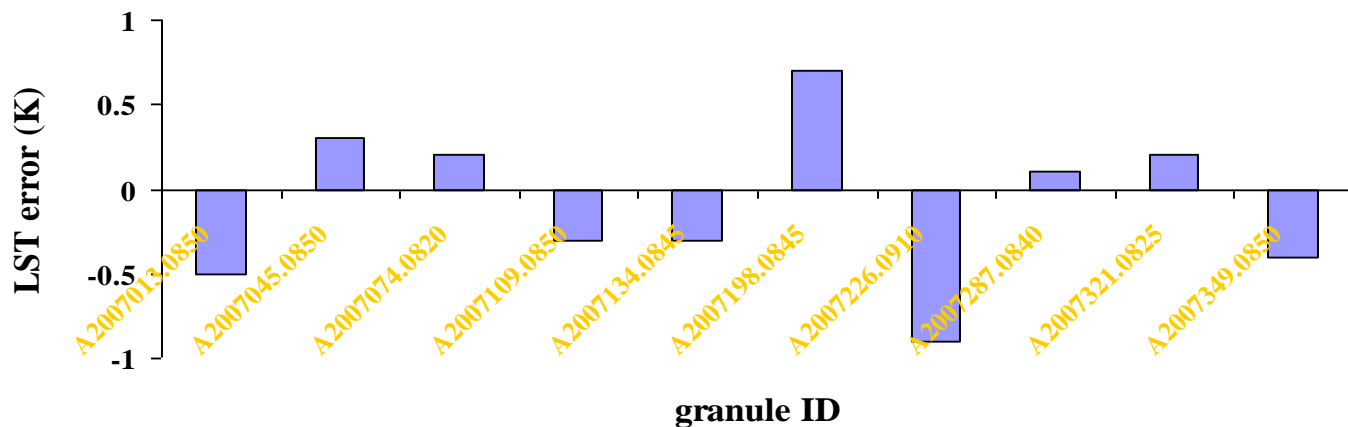


**Radiance-based validation of LSTs in the V5 MOD11_L2 product
at Farafra, Egypt (27.04D N, 27.97D E).
LSTs range from 235-291K.**



with radio
sounding
profiles

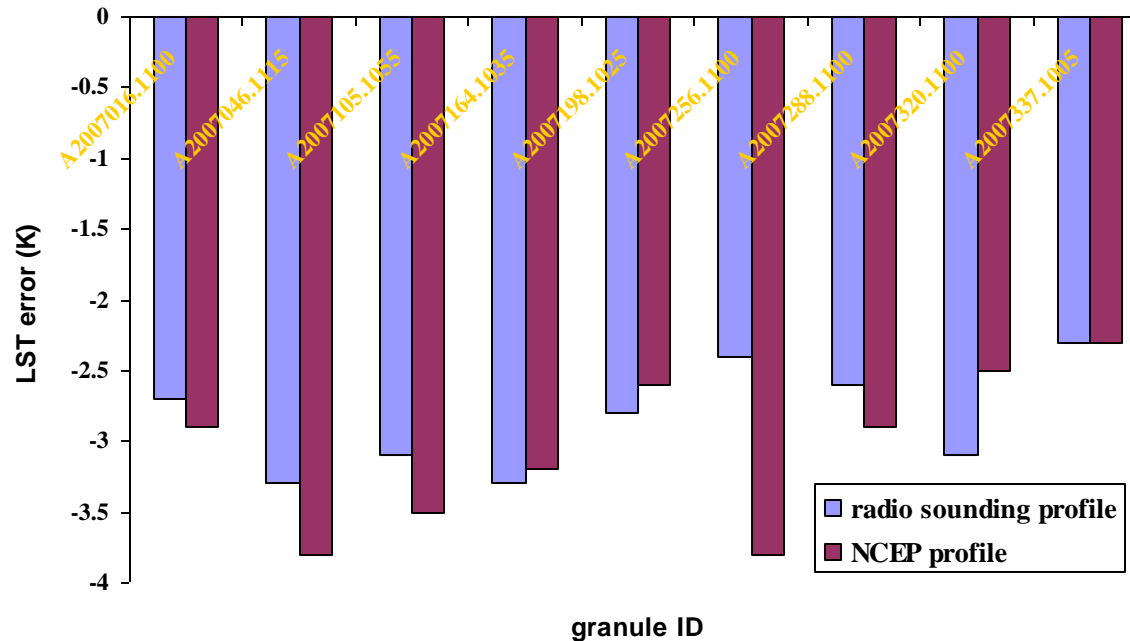
**Radiance-based validation of LSTs in the V5 MOD11_L2 product at
South of Valley University, Egypt (26.2D N, 32.75D E).
Daytime LSTs range from 297-325K.**





How does the V5 split-window algorithm perform in deserts?

R-based validation results of LSTs in the V5 MOD11_L2 product at In-salah, Algeria (27.22°N, 2.5°E) using radio sounding profiles and NCEP modeled profiles.



The mean and standard deviation of LST errors:

$\delta T = 2.8 \pm 0.4K$
when radio sounding profiles
are used, or

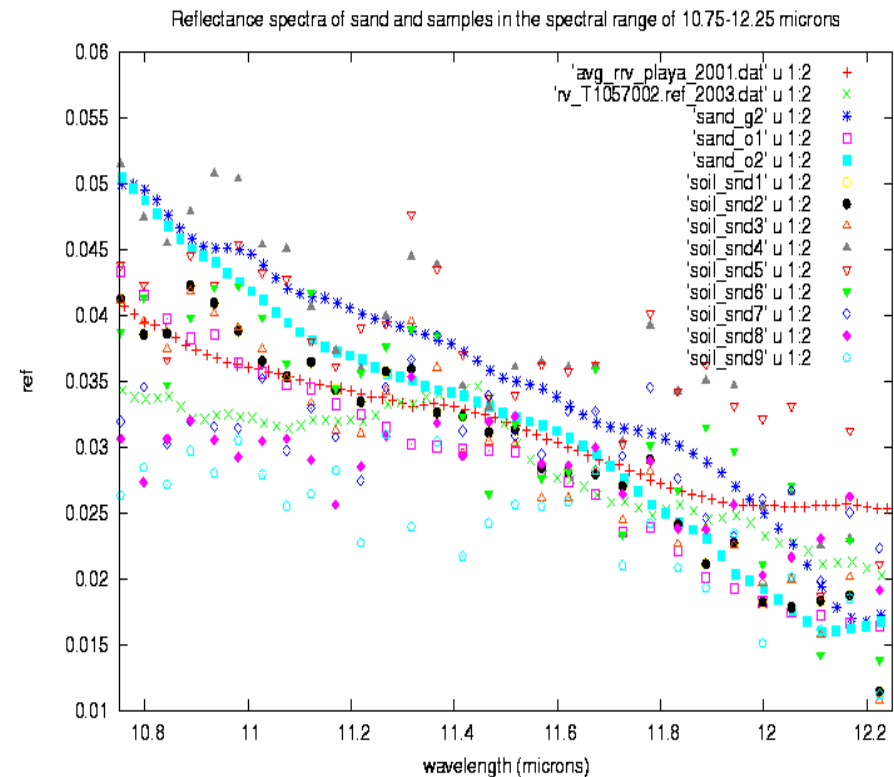
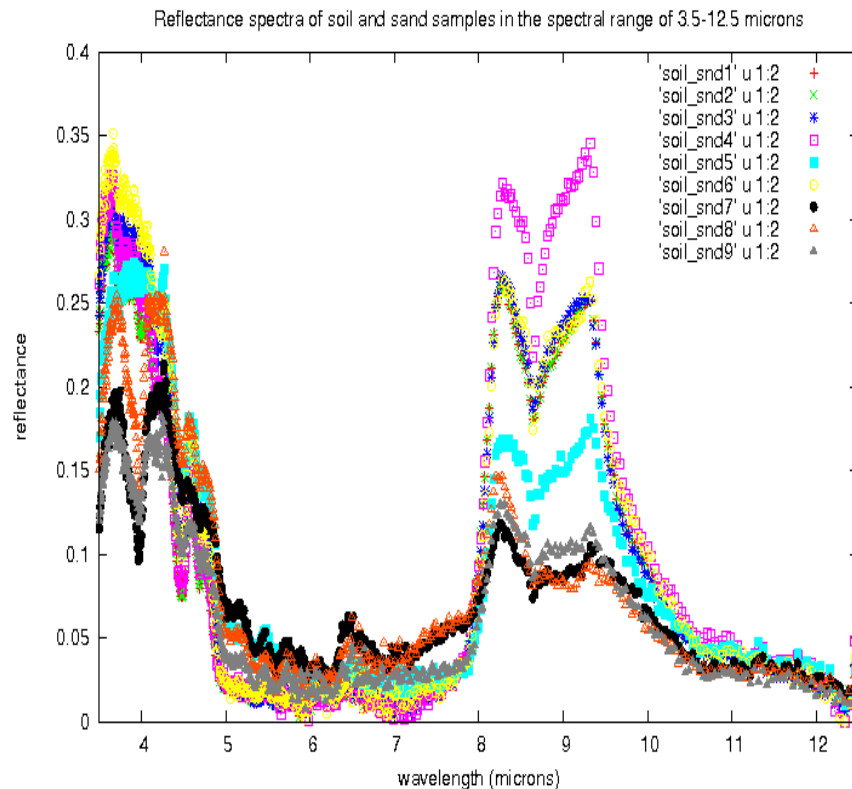
$\delta T = 3.1 \pm 0.5K$
when NCEP modeled profiles
are used.

There is no significant difference in the LSTs at In-salah in the V4 and V5 MOD11A1 products (because the same split-window algorithm has been used in V4 and V5).

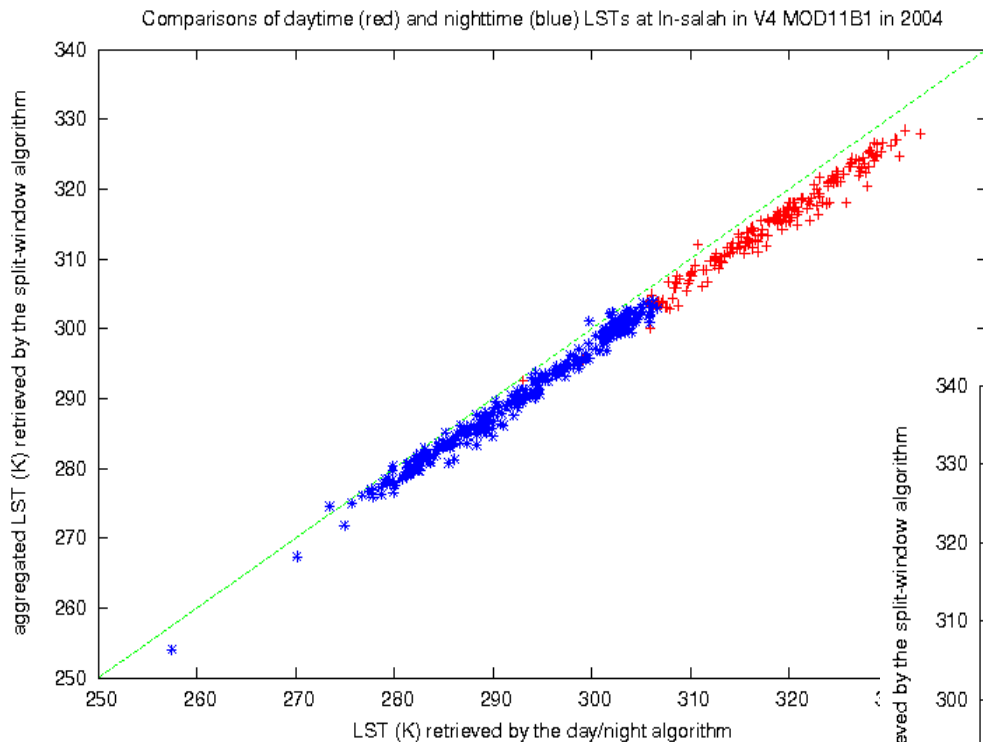
The sensitivity of the split-window algorithm to uncertainties of surface emissivities in bands 31 and 32: if ϵ_{31} reduces by 0.008 and ϵ_{32} increases by 0.008 the retrieved LST value would increase by 2.7K in case of A2007198.1025.



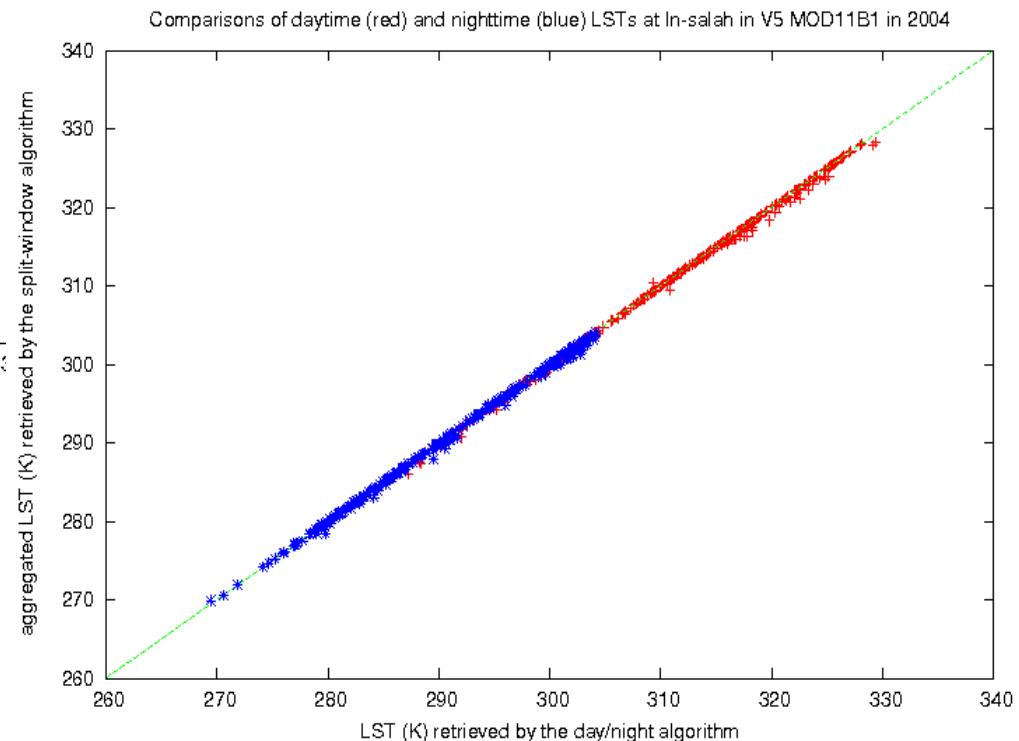
Reflectance spectra measured from sand and soil samples by the MODIS LST group. There are significant variations in the ranges of 3-5 and 8-10 μ m (left) but the change in the reflectance difference in bands 31 and 32 (at 11 and 12 μ m shown in right) may cause large errors in LSTs retrieved by the split-window algorithm



Comparisons of LST values at In-salah (27.22°N, 2.5°E) retrieved by the day/night and split-window algorithms in the V4 and V5 MOD11B1 products in 2004. In V4, the LSTs retrieved by the day/night method is 1-2K larger at night or 2-3K larger and dependent on LST values in daytime.



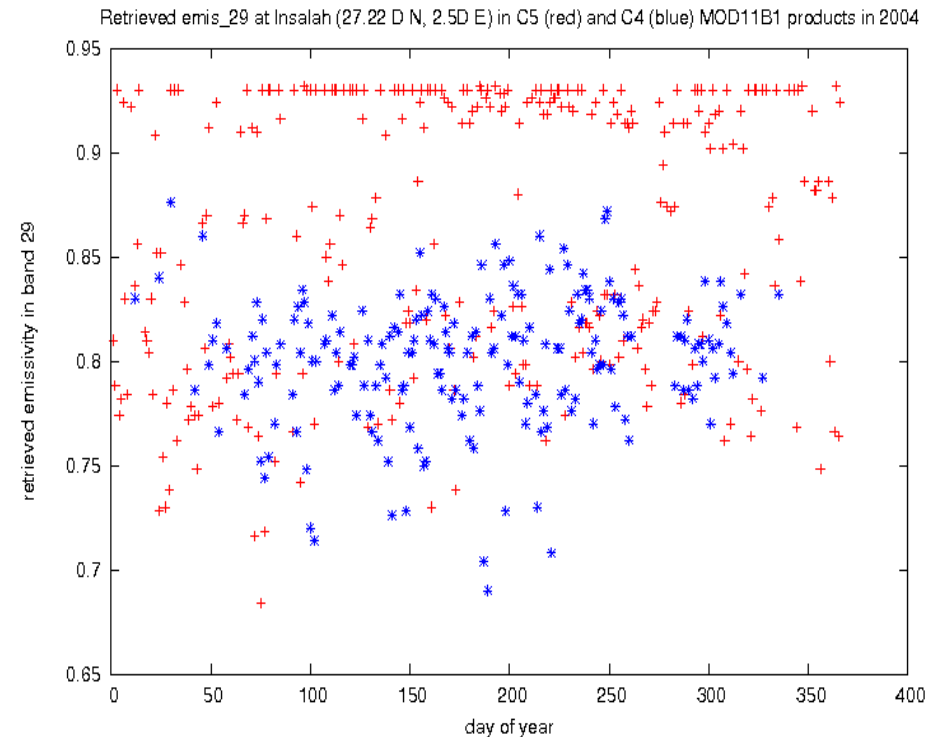
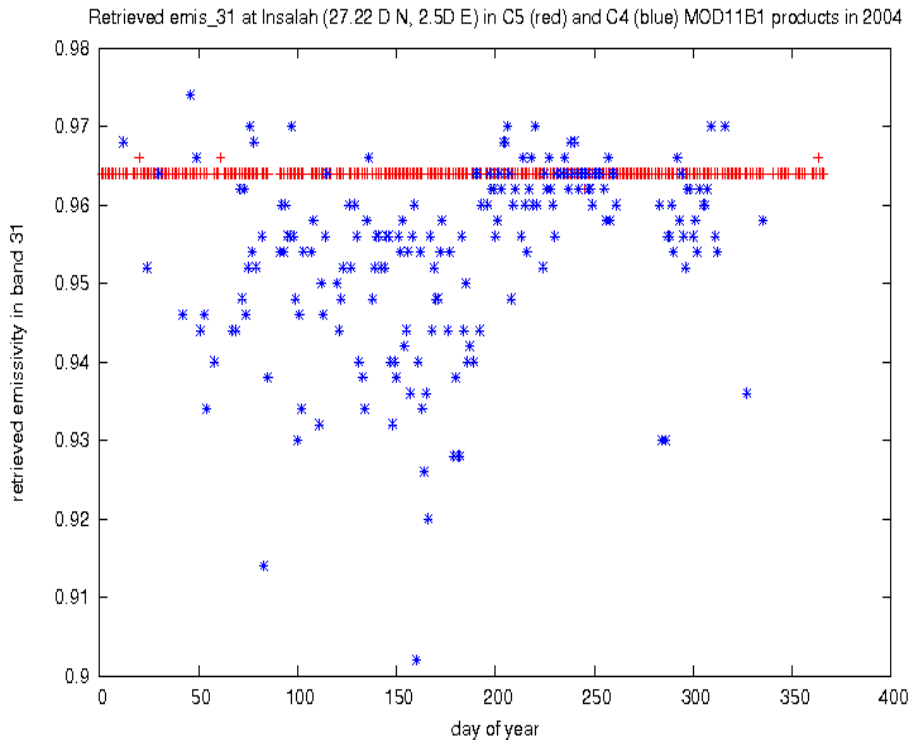
But the V4 day/night algorithm also overestimated LSTs in most regions including lakes and dense vegetation areas. This is not good.



However, the LSTs retrieved by the day/night method are only slightly larger in V5 due to the tight bounding with the split-window method as shown in right.



Comparisons of retrieved surface emissivity values in bands 29 and 31 at In-salah (27.22°N, 2.5°E) in the V4 and V5 MOD11B1 products in 2004. The low fluctuated band-31 values in V4 is bad. The V5 made improvement in band 31 but failed in band 29 due to the large emis29 values above 0.9 in about half cases.



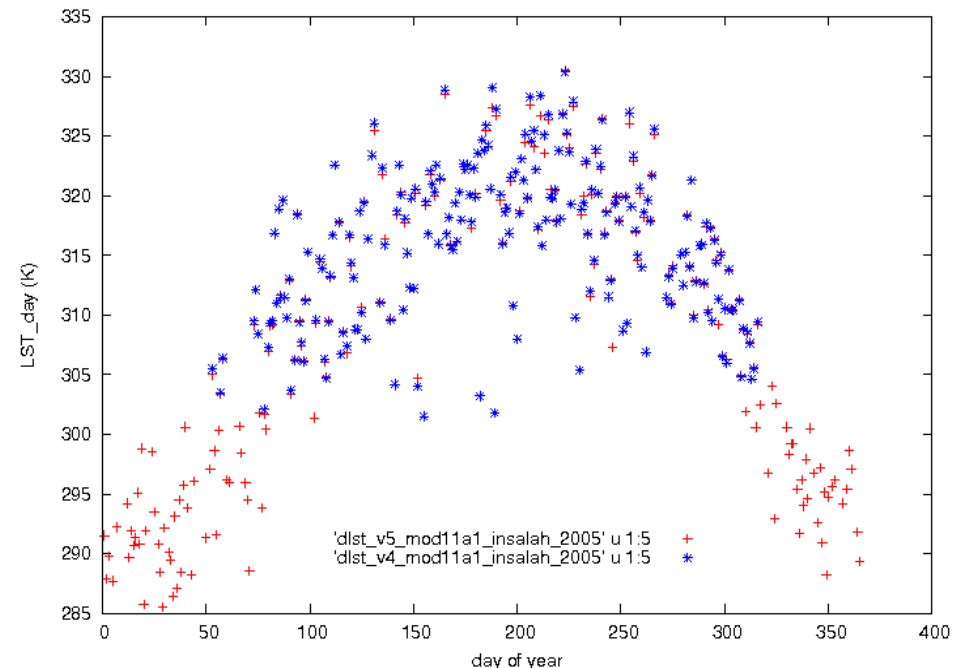


What is wrong with the performance of the V5 day/night algorithm in desert regions?

1. Because the day/night algorithm is tightly bounded with the split-window algorithm in V5, the large errors in LSTs retrieved by the split-window method in desert regions by any reasons also affect the day/night algorithm. So we need to tune the tightness.
2. The definition of clear-sky LSTs in V5 by MOD35 at a confidence of $\geq 95\%$ clear over land $\leq 2000\text{m}$ increased the number of daytime LSTs at In-salah by about 50% both in MOD11A1 and MOD11B1 mainly in spring and winter. This C5 change gives good seasonality in LSTs, as shown in the plot below for day LSTs at In-salah in 2005.

Numbers of days with valid LST values at In-salah in C5 and C4 MOD11A1 and MOD11B1 products in 2004.

product	C5 (V5)	C4 (V4)
MOD11A1 day LST	297	189
MOD11A1 night LST	283	262
MOD11B1 day LST	301	195
MOD11B1 night LST	287	274





Summary of C5 LST Products

1. Daytime and nighttime LSTs in the C5 level-2 Terra & Aqua MODIS LST products (M*D11_L2) retrieved by the split-window algorithm have been validated by the temperature-based approach at large homogeneous sites in lakes, rice field and dense vegetation areas. They have been also validated by the radiance-based approach at various sites in arid regions and cold regions including the South Pole. The LST errors are within 1K in most cases. The LSTs at 6km grids retrieved by the V5 day/night algorithm may be validated indirectly by comparisons to the LSTs from the split-window algorithm aggregated at the 6km grids.
2. The land surface emissivities retrieved by the V5 day/night algorithm have been validated only at a few sites. The large fluctuations in the retrieved emissivities in the desert regions may be due to cloud contaminations and large errors in retrieved LSTs.
3. Cloud contaminations and the effects of aerosols above average loadings are the major source of errors in the MODIS LST products. The affected LSTs in the C5 level-2 MODIS LST products have not been removed although they were removed from the level-3 products.



Proposed Processing Plan for C6 LST Products

- (1), remove cloud-contaminated LSTs not only from level-3 LST products but also from level-2 LST products (MOD11_L2 and MYD11_L2).
- (2), update the coefficient LUT (lst_coef.h) for the split-window algorithm with comprehensive regression analysis of MODIS simulation data in bands 31 and 32 over wide ranges of surface and atmospheric conditions, especially extending the upper boundary for (LST – Ts-air) in arid and semi-arid regions and increasing the overlapping between various sub-ranges in order to reduce the sensitivity of the algorithm to the uncertainties in the input data (i.e., column water vapor and air surface temperature from MOD07 and MYD07).
- (3), make minor adjustments in the classification-based surface emissivity values (band_emis.h), especially for land-cover type of bare soil and rocks.
- (4), tune the day/night algorithm by adjusting weights to improve its performance in desert regions where the incorporated split-window algorithm may not work well.
- (5), generate new LST products for 8-day and monthly at 6km grids (in response to user community requests).



Research Issues for C6 LST Products

(1), add flexibility to input options in the daily PGE16 if the need for near real-time processing capability can be better met without scarifying the LST quality, TBD.

(2), develop methods to analyze and correct the effects of thin cirrus clouds and aerosols above the average loading (the MODIS aerosol product was improved by the deep blue algorithm recently), TBD.

A short list of references



- Wan, Z., (2008). New refinements and validation of the MODIS land-surface temperature/emissivity products. *Remote Sensing of Environment*, 112, 59-74.
- Wan, Z., & Li, Z.-L., (2008). Radiance-based validation for the V5 MODIS land-surface temperature product. *International Journal of Remote Sensing*, to be published in July.
- Wang, K., Wan, Z., Wang, P., Sparrow M., Liu, J., & Haginoya, S., (2007). Evaluation and improvement of the MODIS land surface temperature/emissivity products using ground-based measurements at a semi-desert site on the western Tibetan Plateau. *Int. Journal of Remote Sensing*, 28, 2549-2565
- Coll, C., Caselles, V., Galve, J.M., Valor, E., Niclòs, R., Sánchez, J.M., & Rivas, R. (2005). Ground measurements for the validation of land surface temperatures derived from AATSR and MODIS data. *Remote Sensing of Environment*, 97, 288-300.
- Snyder, W.C., Wan, Z., Zhang, Y., & Feng, Y.-Z. (1998). Classification-based emissivity for land surface temperature measurement from space. *Int. Journal of Remote Sensing*, 19, 2753-2574.
- Wan, Z., & Dozier, J. (1996). A generalized split-window algorithm for retrieving land-surface temperature from space. *IEEE Trans. Geoscience and Remote Sensing*, 34, 892–905.
- Wan, Z., & Li, Z.-L. (1997). A physics-based algorithm for retrieving land-surface emissivity and temperature from EOS/MODIS data. *IEEE Trans. Geoscience and Remote Sensing*, 35, 980-996.
- Li, Z.-L., Becker, F., Stoll, M.P., & Wan, Z (1999). Evaluation of six methods for extracting relative emissivity spectra from thermal infrared images. *Remote Sensing of Environment*, 69, 194-214.
- Wan, Z., Zhang, Y., Zhang, Y.Q., & Li, Z.-L. (2002). Validation of the land-surface temperature products retrieved from Moderate Resolution Imaging Spectroradiometer data. *Remote Sensing of Environment*, 83, 163-180.
- Wan, Z., Zhang, Y., Zhang, Y.Q., & Li, Z.-L. (2004). Quality assessment and validation of the global land surface temperature. *International Journal of Remote Sensing*, 25, 261-274.

<http://www.icess.ucsb.edu/modis/LstUsrGuide/usrguide.html>



Institute for
Computational Earth System Science
University of California, Santa Barbara